UDC 629.5.015:629.544

Ivo SENJANOVIĆ[1]
Šime MALENICA[2]
Stipe TOMAŠEVIĆ[1]
Smiljko RUDAN[1]

Methodology of Ship Hydroelasticity Investigation

Original scientific paper

The importance of hydroelastic analysis of large and flexible container ships of today is pointed out. A methodology for investigation of this challenging phenomenon is drawn up and a mathematical model is worked out. It includes definition of ship geometry, mass distribution, structure stiffness, and combines ship hydrostatics, hydrodynamics, ship motion and vibrations. Based on the presented theory, a computer program is developed and applied for hydroelastic analysis of a flexible segmented barge for which model test results of motion and distortion in waves have been available. A correlation analysis of numerical simulation and measured response shows quite good agreement of the transfer functions for heave, pitch, roll, vertical and horizontal bending and torsion. Such checked tool can be further used for reliable hydroelastic analysis of ship-like structures.

Keywords: *container ships, flexible barge, hydroelasticity, mathematical model, numerical simulation, model tests*

Metodologija istraživanja hidroelastičnosti brodova

Izvorni znanstveni rad

Naglašena je važnost provođenja hidroelastične analize velikih suvremenih kontejnerskih brodova, koji su vrlo elastični u pogledu uvijanja. Opisana je metodologija istraživanja ovog izazovnog problema. Razrađen je matematički model, koji uključuje definiranje geometrije broda, raspodjele masa, krutosti konstrukcije, i objedinjuje hidrostatiku, hidrodinamiku, njihanje i vibracije broda. Na osnovi prikazane teorije razvijena je odgovarajuća programska podrška, koja je primijenjena za hidroelastičnu analizu vrlo elastične segmentne barže, za koju postoje rezultati modelskih ispitivanja njihanja i deformiranja na valovima. Usporedbena analiza numeričke simulacije i izmjerenog odziva pokazala je relativno dobro slaganje prijenosnih funkcija poniranja, posrtanja, ljuljanja, te vertikalnog i horizontalnog savijanja i uvijanja broda. Ovako provjereno sredstvo može se nadalje pouzdano upotrijebiti za hidroelastičnu analizu brodskih konstrukcija.

Ključne riječi: *kontejnerski brodovi, elastična barža, hidroelastičnost, matematički model, numerička simulacija, modelsko ispitivanje*

Authors' addreses:
[1] *University of Zagreb*, Zagreb, Croatia;
e-mail: ivo.senjanovic@fsb.hr
[2] *Bureau Veritas*, Paris, France;
e-mail: sime.malenica@bureauveritas.com

Received (Primljeno): 2007-02-07
Accepted (Prihvaćeno): 2007-03-29
Open for discussion (Otvoreno za raspravu): 2008-06-30

1 Introduction

Sea transport is rapidly increasing and larger fast merchant ships are built. Large ships are relatively more flexible and their structural natural frequencies can fall into the range of the encounter frequencies in an ordinary sea spectrum. Therefore, the wave induced hydroelastic response of large ships becomes an important issue especially for improving the classification rules and ensuring ship safety.

For ships with closed cross-section and ordinary hatch openings such as tankers, bulk carriers, general cargo vessels etc., the lowest natural frequencies are usually associated with the vertical bending. On the other hand, for ships with open cross-section, such as container ships, the lowest elastic natural modes are those of coupled horizontal and torsional vibrations. This coupling is highly pronounced due to the fact that the torsional (shear) centre is below the keel.

The classical approach to determine ship motions and wave loads is based on the assumption that the ship hull acts as a rigid body [1]. The obtained wave load is then imposed to the elastic 3D FEM model of ship structure in order to analyse global longitudinal and transverse strength, as well as local strength with stress concentrations related to fatigue analysis [2].

The above approach is not reliable enough for ultra large ships due to mutual influence of the wave load and structure response. Therefore, a reliable solution requires analysis of wave load and ship vibration as a coupled hydroelastic problem [3]. This is especially important for impulsive loads such as ship slamming that causes whipping.

The methodology of hydroelastic analysis is shown in Figure 1 according [4]. It includes definition of the structural model, ship and cargo mass distributions, and geometrical model of ship surface. First, dry natural vibrations are calculated. Then modal hydrostatic stiffness, modal added mass, damping and wave load are determined. Finally, wet natural vibrations are obtained as well as the transfer functions (RAO-response amplitude operator) for determining ship structural response to wave excitation.

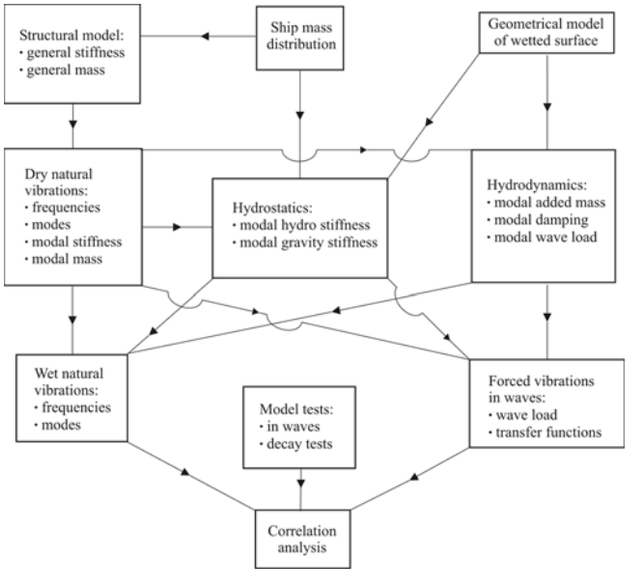

Figure 1 **Methodology of hydroelastic analysis**
Slika 1 **Metodologija hidroelastične analize**

2 Structural model

The hydroelastic problem can be solved at different levels of complexity and accuracy. The best, but highly time-consuming way is to consider 3D FEM structural model and 3D hydrodynamic model based on the radiation-diffraction theory [5]. Such an approach is recommended only for the final strength analysis. However, in the preliminary strength analysis it is more rational and convenient to couple 1D FEM model of ship hull [6] with 3D hydrodynamic model.

In both cases of the FEM approach the governing matrix equation of dry natural vibrations yields [7]

$$\left([\mathbf{K}]-\Omega^2[\mathbf{M}]\right)\{\delta\}=\{0\} \tag{1}$$

where

$[\mathbf{K}]$ - stiffness matrix
$[\mathbf{M}]$ - mass matrix
Ω - dry natural frequency
$\{\delta\}$ - dry natural mode

As solution of the eigenvalue problem (1) Ω_i and $\{\delta\}_i$ are obtained for each the i-th dry mode, where $i = 1,2...N$, N is total number of degrees of freedom. Now natural modes matrix can be constituted

$$[\delta]=\left[\{\delta\}_1,\{\delta\}_2\ldots\{\delta\}_i\ldots\{\delta\}_N\right] \tag{2}$$

and the modal stiffness and mass can be determined [8]

$$[\mathbf{k}]=[\delta]^T[\mathbf{K}][\delta],\quad [\mathbf{m}]=[\delta]^T[\mathbf{M}][\delta] \tag{3}$$

Since the dry natural vectors are mutually orthogonal, matrices $[\mathbf{k}]$ and $[\mathbf{m}]$ are diagonal. Terms k_i and $\Omega_i^2 m_i$ represent deformation and kinetic energy of the i-th mode respectively.

Note that generally the first six natural frequencies Ω_i are zero with corresponding eigenvectors representing the rigid body modes. As a result, the first six diagonal elements of $[\mathbf{k}]$ are also zero, while the first three elements in $[\mathbf{m}]$ are equal to structure mass, the same in all directions x, y, z, and the next three elements represent the mass moment of inertia around the coordinate axes.

3 Geometrical model of wetted surface

3.1 Strip mesh

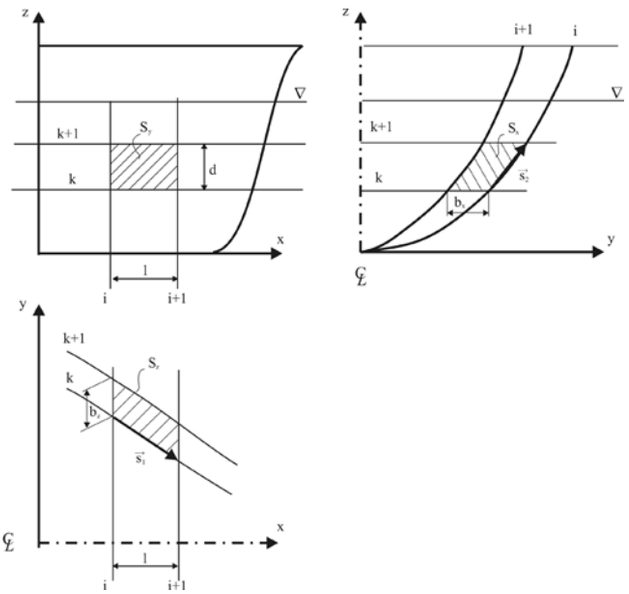

Figure 2 **Panel of wetted surface**
Slika 2 **Panel oplakane površine**

For determining pressure forces acting on the wetted surface it is necessary to specify panels and their position in space. Wet surface is given by offsets of waterline ordinates at body plan stations, b_{ik}. If the strip method is used for pressure calculation, then the panels bounded with two close stations, i and $i + 1$, and waterplanes, k and $k + 1$, can be used, Figure 2. Arcs of the panel yield

$$\mathbf{s}_1 = l\mathbf{i}+b_x\mathbf{j},\quad \mathbf{s}_2 = b_z\mathbf{j}+d\mathbf{k} \tag{4}$$

where

$b_x = b_{i+1,k} - b_{i,k}$, $b_z = b_{i,k+1} - b_{i,k}$
l - station distance
d - waterplane distance

The panel normal vector is

$$\mathbf{n}=\frac{\mathbf{S}}{S}=\frac{\mathbf{s}_1\times\mathbf{s}_2}{|\mathbf{s}_1\times\mathbf{s}_2|}=n_x\mathbf{i}+n_y\mathbf{j}+n_z\mathbf{k} \tag{5}$$

with components

$$n_x=\frac{db_x}{S},\quad n_y=-\frac{ld}{S},\quad n_z=\frac{lb_z}{S} \tag{6}$$

where

$$S = \sqrt{(db_x)^2 + (ld)^2 + (lb_z)^2} = \sqrt{S_x^2 + S_y^2 + S_z^2} \qquad (7)$$

is the panel area.

3.2 Rational mesh

If 3D radiation-diffraction theory is used for hydrodynamic pressure determination, the wetted surface mesh can be created in such a way that panels of more regular shape and refined subdivision in the area of the free surface are achieved [9]. Such a rational mesh is shown in Figure 3, where the panel rows follow the ship body diagonals similarly to the structural elements of ship outer shell. In this way, efficiency and accuracy of the hydrodynamic calculation is increased.

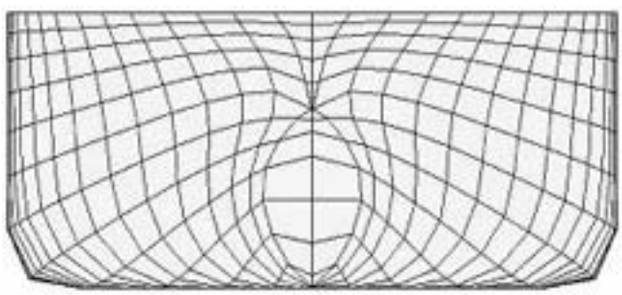

Figure 3 **Rational mesh of wetted surface**
Slika 3 **Racionalna mreža oplakane površine**

Concerning the normal vector, let us consider a triangular panel, which is defined by three position vectors from the origin of the coordinate system x, y, z

$$\mathbf{r}_i = x_i\mathbf{i} + y_i\mathbf{j} + z_i\mathbf{k}, \quad i = 1,2,3 \qquad (8)$$

The panel arcs are

$$\mathbf{a} = \mathbf{r}_2 - \mathbf{r}_1, \quad \mathbf{b} = \mathbf{r}_3 - \mathbf{r}_1 \qquad (9)$$

and the panel normal vector yields

$$\mathbf{n} = \frac{\mathbf{S}}{S} = \frac{\mathbf{a}\times\mathbf{b}}{|\mathbf{a}\times\mathbf{b}|} = n_x\mathbf{i} + n_y\mathbf{j} + n_z\mathbf{k} \qquad (10)$$

where S is double value of the triangular panel area.

4 Dry modes of wetted surface

As mentioned in Section 2, structural dry modes can be determined by 1D or 3D FEM analysis. If 1D analysis is used, the beam modes are spread to the ship wetted surface as follows.

Vertical vibration

$$\mathbf{h}_v = -\frac{\mathrm{d}\,w_h}{\mathrm{d}\,x}(Z - z_N)\mathbf{i} + w_v\mathbf{k} \qquad (11)$$

Horizontal vibration

$$\mathbf{h}_h = -\frac{\mathrm{d}\,w_h}{\mathrm{d}\,x}Y\,\mathbf{i} + w_h\,\mathbf{j} \qquad (12)$$

Torsional vibration

$$\mathbf{h}_t = \psi\,(Z - z_S)\,\mathbf{j} - \psi\,Y\,\mathbf{k} \qquad (13)$$

where w is hull deflection, ψ is twist angle, Y and Z are coordinates of the point on ship surface, and z_N and z_S are coordinates of neutral line and shear centre respectively.

If strong coupling between horizontal and torsional vibration occurs, as in the case of container ships, the coupled mode yields

$$\mathbf{h}_{ht} = \left(-\frac{\mathrm{d}\,w_h}{\mathrm{d}\,x}Y + \frac{\mathrm{d}\,\psi}{\mathrm{d}\,x}\bar{u}\right)\mathbf{i} + \left[w_h + \psi\,(Z - z_S)\right]\mathbf{j} - \psi\,Y\,\mathbf{k} \qquad (14)$$

where $\bar{u} = \bar{u}(x, Y, Z)$ is the cross-section warping function reduced to the wetted surface [10], [11].

5 Hydrodynamic model

Harmonic hydroelastic problem is considered in frequency domain and therefore we operate with amplitudes of forces and displacement. In order to perform coupling of the structural and hydrodynamic models, it is necessary to express the external pressure forces in a convenient manner [12]. First, the total hydrodynamic force F^h has to be split into two parts: the first part F^R depending on the structural deformations, and the second one F^{DI} representing the pure excitation

$$F^h = F^R + F^{DI} \qquad (15)$$

Furthermore, the modal superposition method can be used. Vector of the wetted surface deformations $\mathbf{H}(x, y, z)$ can be presented as a series of dry natural modes $\mathbf{h}_i(x, y, z)$

$$\mathbf{H}(x,y,z) = \sum_{i=1}^{N}\xi_i\,\mathbf{h}_i(x,y,z) = \\ = \sum_{i=1}^{N}\xi_i\left[h_x^i(x,y,z)\mathbf{i} + h_y^i(x,y,z)\,\mathbf{j} + h_z^i(x,y,z)\mathbf{k}\right] \qquad (16)$$

where ξ_i are unknown coefficients. Vectors $\mathbf{h}_i(x, y, z)$ related to wetted surface are obtained from the structural dry modes as explained in the previous section.

The potential theory assumptions are adopted for the hydrodynamic part of the problem. Within this theory the total velocity potential φ, in the case of no forward speed, is defined with the Laplace differential equation and the given boundary values

$$\begin{aligned} &\Delta\varphi = 0 && \text{within the fluid} \\ &-\nu\varphi + \frac{\partial\varphi}{\partial z} = 0 && \text{at the free surface, } z = 0 \\ &\frac{\partial\varphi}{\partial n} = -i\omega\,\mathbf{H}\,\mathbf{n} && \text{on the wetted body surface, } S \end{aligned} \qquad (17)$$

where ν is the wave number, $\nu = \omega^2/g$, ω is wave frequency, $\mathbf{n}$ is the wetted surface normal vector, and i is the imaginary unit [13].

Furthermore, the linear wave theory enables the following decomposition of the total potential [5]

$$\varphi = \varphi_I + \varphi_D - i\omega \sum_{j=1}^{N} \xi_j \varphi_{Rj} \tag{18}$$

where

$$\varphi_I = -i \frac{gA}{\omega} \mathrm{e}^{\nu(z+ix)} \tag{19}$$

φ_I - incident wave potential
φ_D - diffraction potential
φ_{Rj} - radiation potential
A - wave amplitude

Now, the body boundary conditions (17) can be deduced for each potential

$$\frac{\partial \varphi_D}{\partial n} = -\frac{\partial \varphi_I}{\partial n}, \quad \frac{\partial \varphi_{Rj}}{\partial n} = \mathbf{h}_j \mathbf{n} \tag{20}$$

It is necessary to point out that the diffraction and radiation potentials should also satisfy the radiation condition at infinity.

Once the potentials are determined, the modal hydrodynamic forces are calculated by pressure work integration over the wetted surface. The total linearised pressure can be found from Bernoulli's equation

$$p = i\omega\rho\varphi - \rho g z \tag{21}$$

First, the term associated with the potential φ is considered and subdivided into excitation and radiation parts (18)

$$F_i^{DI} = i\omega\rho \iint_S (\varphi_I + \varphi_D)\mathbf{h}_i \mathbf{n}\, \mathrm{d}S \tag{22}$$

$$F_i^R = \rho\omega^2 \sum_{j=1}^{N} \xi_j \iint_S \varphi_{Rj} \mathbf{h}_i \mathbf{n}\, \mathrm{d}S \tag{23}$$

Thus, (22) represents the modal pressure excitation. Now one can decompose (23) into the modal inertia force and damping force associated with acceleration and velocity respectively

$$F_i^a = \mathrm{Re}(F_i^R) = \omega^2 \sum_{j=1}^{N} \xi_j A_{ij}, \quad A_{ij} = \rho\, \mathrm{Re} \iint_S \varphi_{Rj}\, \mathbf{h}_i \mathbf{n}\, \mathrm{d}S \tag{24}$$

$$F_i^v = i\, \mathrm{Im}(F_i^R) = i\omega \sum_{j=1}^{N} \xi_j B_{ij}, \quad B_{ij} = \rho\omega\, \mathrm{Im} \iint_S \varphi_{Rj}\, \mathbf{h}_i \mathbf{n}\, \mathrm{d}S \tag{25}$$

where A_{ij} and B_{ij} are elements of added mass and damping matrices respectively.

Determination of added mass and damping for rigid body modes is a well-known procedure in ship hydrodynamics [1]. Now the same procedure is extended to the calculation of these quantities for elastic modes.

The hydrostatic part of the total pressure, $-\rho g z$ in (21), is considered within the hydrostatic model.

6 Hydrostatic model

6.1 Elastic modes

General

In dynamic analysis a structure vibration is considered with respect to the static equilibrium position. Therefore, only dynamic forces, i.e. inertia, damping, restoring and excitation ones are taken into account. Time independent forces are included in still water strength analysis as a separated static problem. Dynamic analysis is performed by the modal superposition method. Modal forces represent work of actual forces on modal displacements. Modal restoring forces consist of time dependent modal pressure forces and gravity forces. They include effect of large displacements.

Pressure forces

Concerning the hydrostatic part of the total pressure in (21), $\rho g z$, it is necessary to determine the change of the modal hydrostatic force as the difference between its instantaneous value and the initial value for the vibration mode $\mathbf{h}_i$ of the body wetted surface $Z = Z(x, y)$ [14]

$$F_i^H = -\rho g \iint_{\tilde{S}} \tilde{Z}\, \tilde{\mathbf{h}}_i\, \tilde{\mathbf{n}}\, \mathrm{d}\tilde{S} + \rho g \iint_S Z \mathbf{h}_i \mathbf{n}\, \mathrm{d}S \tag{26}$$

Each of the above quantities can be presented in the form $\tilde{(...)} = (...) + \delta(...)$, where δ denotes the variation. By neglecting small terms of higher order, one can write for the modal hydrostatic force (26)

$$F_i^H = -\rho g \iint_S (\delta Z\, \mathbf{h}_i\, \mathbf{n} + Z\, \delta \mathbf{h}_i\, \mathbf{n} + Z \mathbf{h}_i\, \delta \mathbf{n}) \mathrm{d}S \tag{27}$$

Variation of the particular quantity can be determined by applying the notion of directional derivative $\mathbf{H}\nabla$, where $\mathbf{H}$ is given with (16) and ∇ is Hamilton differential operator

$$\mathbf{H}\nabla = \sum_{j=1}^{N} \xi_j \mathbf{h}_j \nabla = \sum_{j=1}^{N} \xi_j \left(h_x^j \frac{\partial}{\partial x} + h_y^j \frac{\partial}{\partial y} + h_z^j \frac{\partial}{\partial z} \right) \tag{28}$$

As a result

$$\delta Z = (\mathbf{H}\nabla)Z = \mathbf{H}\mathbf{k}, \quad \delta \mathbf{h}_i = (\mathbf{H}\nabla)\mathbf{h}_i, \quad \delta \mathbf{n} = (\mathbf{H}\nabla)\mathbf{n} \tag{29}$$

Determining the variation of the body surface normal vector, $\delta\mathbf{n}$, according to (29) is a rather difficult task. Therefore, a relatively simpler procedure, taken from [14], is shown in Appendix A.

By using Eqs. (28), (29) and (A12), the modal hydrostatic force (27) can be presented in the following form:

$$F_i^H = -\sum_{j=1}^{N} \xi_j C_{ij}^H \tag{30}$$

where

$$C_{ij}^H = C_{ij}^{Hp} + C_{ij}^{Hh} + C_{ij}^{Hn} \tag{31}$$

is the i,j-th element of the hydrostatic stiffness matrix, composed of static pressure, surface mode and normal vector contributions, respectively

$$C_{ij}^{Hp} = \rho g \iint_S h_z^j (h_x^i n_x + h_y^i n_y + h_z^i n_z) \mathrm{d}S \tag{32}$$

$$C_{ij}^{Hh} = \rho g \iint_S Z \left[\left(h_x^j \frac{\partial h_x^i}{\partial x} + h_y^j \frac{\partial h_x^i}{\partial y} + h_z^j \frac{\partial h_x^i}{\partial z} \right) n_x + \right.$$
$$+ \left(h_x^j \frac{\partial h_y^i}{\partial x} + h_y^j \frac{\partial h_y^i}{\partial y} + h_z^j \frac{\partial h_y^i}{\partial z} \right) n_y + \qquad (33)$$
$$\left. + \left(h_x^j \frac{\partial h_z^i}{\partial x} + h_y^j \frac{\partial h_z^i}{\partial y} + h_z^j \frac{\partial h_z^i}{\partial z} \right) n_z \right] \mathrm{d}S$$

$$C_{ij}^{Hn} = \rho g \iint_S Z \left\{ \left[\left(\frac{\partial h_y^j}{\partial y} + \frac{\partial h_z^j}{\partial z} \right) n_x - \frac{\partial h_y^j}{\partial x} n_y - \frac{\partial h_z^j}{\partial x} n_z \right] h_x^i + \right.$$
$$+ \left[-\frac{\partial h_x^j}{\partial y} n_x + \left(\frac{\partial h_x^j}{\partial x} + \frac{\partial h_z^j}{\partial z} \right) n_y - \frac{\partial h_z^j}{\partial y} n_z \right] h_y^i + \qquad (34)$$
$$\left. + \left[-\frac{\partial h_x^j}{\partial z} \boldsymbol{n}_x - \frac{\partial h_y^j}{\partial z} n_y + \left(\frac{\partial h_x^j}{\partial x} + \frac{\partial h_y^j}{\partial y} \right) n_z \right] h_z^i \right\} \mathrm{d}S$$

Note that the wetted surface coordinate Z is measured from the waterplane. Based on the constitution of the above coefficients, it is evident that the hydrostatic stiffness matrix is not diagonal.

In the literature various definitions of hydrostatic stiffness matrix can be found. Somewhat simple formulae are derived in [15] using a slightly different approach. Those formulae lead to the same result as the more classical method in which some integral transformations are applied in order to simplify the final expressions [16], as elaborated in [15]. Quite different expressions are presented in [17].

The advantage of the present method is that the derived formulae are general and applicable for a complex body as well as for its parts. This is important for determining the local hydrostatic action as internal loads, transfer of load to a FEM structural model, etc.

If 1D structural model is used together with the strip mesh, the integration over the body wetted surface in determining the hydrostatic stiffness (32), (33) and (34) can be split into two steps

$$\iint_S F(x,y,z)\mathrm{d}S = \int_0^L f(x) \int_s g(x,s)\mathrm{d}s\,\mathrm{d}x \qquad (35)$$

where $f(x)$ is modal function, $g(x, s)$ is function of modal coefficients and s is circumference coordinate of body station.

Gravity forces

The above expressions represent only the action of the hydrostatic pressure, and the gravity part has to be added in order to complete the total restoring coefficients. Similarly to the pressure part, Eqs. (26) and (27), a change of the generalised modal gravity force associated with a particular mode yields [14]

$$F_i^m = -g \iiint_V \delta \mathbf{h}_i \mathbf{k}\, \mathrm{d}m \qquad (36)$$

where V is body volume and dm is differential mass.

By employing (29) and further (28) one can write

$$F_i^m = -g \iiint_V (\mathbf{H}\nabla) h_z^i \,\mathrm{d}m = -\sum_{j=1}^{N} \xi_j C_{ij}^m \qquad (37)$$

where

$$C_{ij}^m = g \iiint_V \left(h_x^j \frac{\partial h_z^i}{\partial x} + h_y^j \frac{\partial h_z^i}{\partial y} + h_z^j \frac{\partial h_z^i}{\partial z} \right) \mathrm{d}m \qquad (38)$$

Restoring stiffness

Finally, the complete restoring coefficients read

$$C_{ij} = C_{ij}^H + C_{ij}^m \qquad (39)$$

It is important to point out that the above expressions for the hydrostatic and gravity coefficients are general and therefore valid not only for the elastic modes but also for the rigid body modes as well as for their coupling.

6.2 Rigid body modes

In this special case, the modal restoring stiffness can be determined in direct, simpler and physically more understandable manner. It can also be used for checking the previously developed general method.

A free ship exhibits rigid body motion with six degrees of freedom around its centre of gravity. The first three rigid body modes are unit translations in direction of the coordinate axes, while the other three are unit rotations around these axes. The modal restoring stiffness is equal to the restoring force or moment per unit displacement respectively. According to the ship hydrostatics only three degrees of freedom have restoring force [1]

Heave:

$$C_{33} = \rho g A_{WL} \qquad (40)$$

Roll:

$$C_{44} = \rho g \left[I_{WLX} + V(z_B - z_G) \right] \qquad (41)$$

Pitch:

$$C_{55} = \rho g \left[I_{WLY} + V(z_B - z_G) \right] \qquad (42)$$

where

- A_{WL} - waterplane area
- I_{WLX} - transverse moment of inertia of waterplane area
- I_{WLY} - longitudinal moment of inertia of waterplane area
- V - volume of displacement
- z_B, z_G - coordinate of centre of buoyancy and centre of gravity respectively (from base line).

When rigid body modes are in question, it is also necessary to determine modal ship mass. For the translations, modal masses are equal to the total ship mass, while for the rotations, modal masses represent ship mass moments of inertia around coordinate axes.

7 Hydroelastic model

After the structural, hydrostatic and hydrodynamic models have been determined, the hydroelastic model can be constituted. For that purpose, let us impose modal hydrodynamic forces (23), (24) and (25) and hydrostatic and gravity forces (30), (36) to the modal structural model, Section 2.

$$\left(\left[\mathbf{k}\right]-\omega^2\left[\mathbf{m}\right]\right)\left\{\xi\right\}=\left\{\mathbf{F}\right\}^{DI}+\left\{\mathbf{F}\right\}^{a}+\left\{\mathbf{F}\right\}^{v}+\left\{\mathbf{F}\right\}^{H}+\left\{\mathbf{F}\right\}^{m} \quad (43)$$

Furthermore, all terms dependent on unknown modal amplitudes, ξ_i, can be separated on the left hand side. Thus, the governing matrix differential equation for ship motions and vibrations is deduced

$$\left\{\left[\mathbf{k}\right]+\left[\mathbf{C}\right]-i\omega\left(\left[\mathbf{d}\right]+\left[\mathbf{B}(\omega)\right]\right)-\omega^2\left(\left[\mathbf{m}\right]+\left[\mathbf{A}(\omega)\right]\right)\right\}\left\{\xi\right\}=\left\{\mathbf{F}\right\} \quad (44)$$

where all quantities are related to the dry modes

- $[\mathbf{k}]$ - structural stiffness
- $[\mathbf{d}]$ - structural damping
- $[\mathbf{m}]$ - structural mass
- $[\mathbf{C}]$ - restoring stiffness
- $[\mathbf{B}(\omega)]$ - hydrodynamic damping
- $[\mathbf{A}(\omega)]$ - added mass
- $\{\xi\}$ - modal amplitudes
- $\{\mathbf{F}\}$ - wave excitation
- ω - encounter frequency

Structural damping can be given as a percentage of the critical value based on experience. As it is well-known, added mass and hydrodynamic damping depends on the frequency. The solution of (44) gives the modal amplitudes ξ_i and displacement of any point of the structure obtained by retracking to (16).

The wet natural modes can also be determined by solving the eigenvalue problem extracted from (44)

$$\left\{\left[\mathbf{k}\right]+\left[\mathbf{C}\right]-\omega^2\left(\left[\mathbf{m}\right]+\left[\mathbf{A}(\omega)\right]\right)\right\}\left\{\xi\right\}=\left\{0\right\} \quad (45)$$

Now damping is neglected since its influence on the eigenpair is very small. The solution of (45) gives natural frequencies of ship motion and vibration in water and the corresponding so-called wet natural modes. Since added mass is a frequency dependent function, it is evident that an iteration procedure has to be employed to solve (45). Therefore, the wet modes are not orthogonal. Also, there are no more zero natural frequencies and pure rigid body modes due to their coupling with the elastic modes [12].

8 Hydroelasticity of a flexible barge

8.1 Barge characteristics

The experimental model of a flexible barge, consisting of 12 pontoons, is considered [4], [12]. The front pontoon No. 12 differs somewhat from the others. The pontoons are connected by a steel rod somewhat above the deck level, as shown in Figure 4. So, the deformation centre is above the gravity centre. This is the opposite situation to the one in the case of container ships, but anyway strong coupling between horizontal and torsional vibrations is achieved.

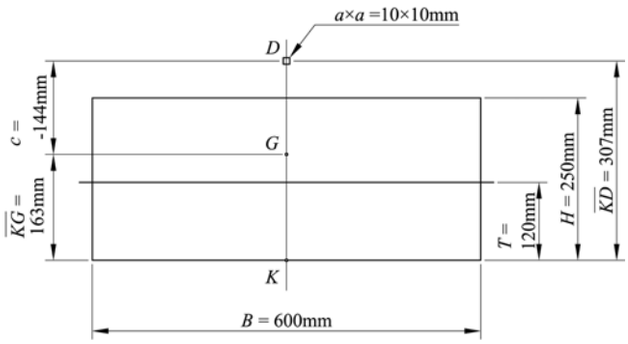

Figure 4 **Barge cross-section**
Slika 4 **Poprečni presjek barže**

The main characteristics of the prismatic barge are the following [4], [12]:

Young's modulus of rod: $E = 2.1 \cdot 10^{11}$ N/m^2
Shear modulus of rod: $G = 0.808 \cdot 10^{11}$ N/m^2
Moment of inertia of rod cross-section: $I_y = I_z = \frac{a^4}{12} = 8.33 \cdot 10^{-10}$ m^4
Polar moment of inertia of rod cross-section: $I_t = \frac{a^4}{6} = 16.67 \cdot 10^{-10}$ m^4
Bending stiffness of rod: $EI = 175$ Nm^2
Torsional stiffness of rod: $GI_t = 135$ Nm^2
Length of barge (pontoons + clearances): $L = 2.445$ m
Total mass (pontoons + equipment): $M = 171.77$ kg
Distributed mass: $m = M/L = 70.253$ kg/m
Radius of gyration in roll: $i_x = 0.225$ m
Polar moment of inertia of distributed mass: $J_t^0 = mi_x^2 = 3.556$ kgm
Distance of gravity centre from torsional centre: $c = -0.144$ m
Polar mass moment of inertia about torsional centre: $J_t = J_t^0 + mz^2 = 5.013$ kgm
Radius of inertia: $r = \sqrt{\frac{J_t}{m}} = 0.267$ m

8.2 Dry vibrations

Dry vertical natural vibration and coupled horizontal and torsional vibrations are performed by a general computer program developed for this purpose [18]. The program is based on the theory presented in [6]. As a result of dry vibration calculation the modal stiffness and modal mass in (44) are obtained. The first two natural modes are shown in Figures 5 and 6.

Natural vibrations for a prismatic pontoon can be also determined analytically as elaborated in [19].

Vertical vibration, $-l \le x \le l$, $\quad l = L/2$
Symmetric modes

$$w_n = \frac{1}{2}\left(\frac{\mathrm{ch}\beta_n x}{\mathrm{ch}\beta_n l}+\frac{\cos\beta_n x}{\cos\beta_n l}\right), \quad n = 0, 2, 4... \quad (46)$$

$\beta_0 l = 0, \qquad \beta_2 l = 2.365, \qquad \beta_4 l = 5.497$

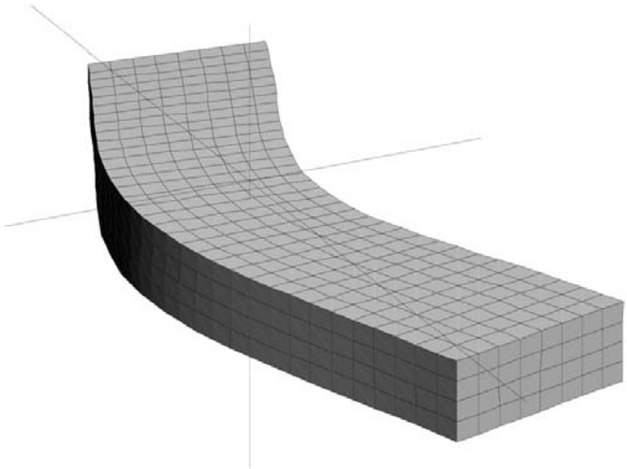

Figure 5 **The first dominant flexural mode of coupled barge vibrations, ω_2 = 5.727 rad/s**
Slika 5 **Prvi pretežno fleksijski oblik spregnutih vibracija barže, ω_2 = 5.727 rad/s**

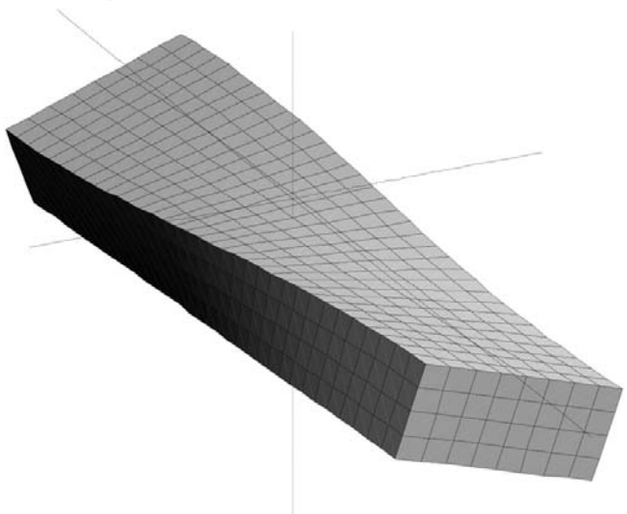

Figure 6 **The first dominant torsional mode of coupled barge vibrations, ω_3 = 7.884 rad/s**
Slika 6 **Prvi pretežno torzijski oblik spregnutih vibracija barže, ω_3 = 7.884 rad/s**

Anti-symmetric modes

$$w_n = \frac{1}{2}\left(\frac{\mathrm{sh}\beta_n x}{\mathrm{sh}\beta_n l} + \frac{\sin\beta_n x}{\sin\beta_n l}\right), \quad n = 1, 3, 5... \tag{47}$$

$$\beta_1 l = 0, \qquad \beta_3 l = 3.925, \qquad \beta_5 l = 7.068$$

where

$$\omega_n = \frac{(\beta_n l)^2}{l^2}\sqrt{\frac{EI}{m}} \tag{48}$$

Analytical solution of coupled horizontal and torsional vibrations can be obtained by direct integration of governing differential equations or by the energy approach. However, in both cases the solution is rather complicated [19].

8.3 Hydrostatic and hydrodynamic parameters

Restoring stiffness matrix in (44) is determined by the developed program [18] based on the theory considered in Section 6. However, for better understanding of the physical meaning, the calculation procedure is illustrated in Appendix B for the case of vertical vibration of the prismatic barge.

Added mass, hydrodynamic damping and wave excitation in (44), depending on dry modes and wave frequency, are determined by program Hydrostar [20]. Structural damping of the pontoon joints to the rod, and of the rod itself is quite low in the considered case. The mesh of the wetted surface used in the calculation is shown in Figure 7.

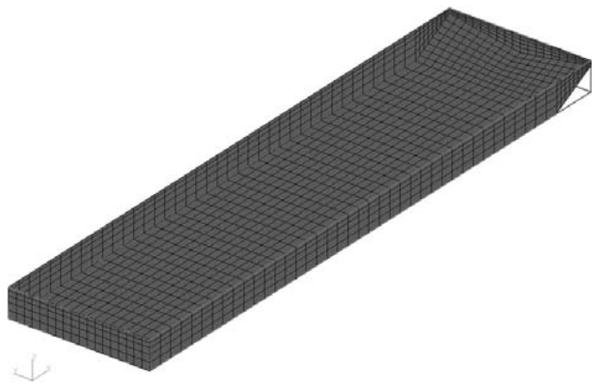

Figure 7 **Geometrical model of barge wetted surface**
Slika 7 **Geometrijski model oplakane površine barže**

All necessary vibration parameters are determined for a set of dry modes consisting of 6 rigid body modes, the first 5 vertical elastic modes and 5 coupled horizontal and torsional modes. The chosen number of elastic modes is sufficient to describe accurately enough the barge response in waves.

8.4 Barge response

The model tests of the considered barge were conducted in the BGO-First Basin, Toulon, France. Detailed description of

Figure 8 **Barge in waves**
Slika 8 **Barža na valovima**

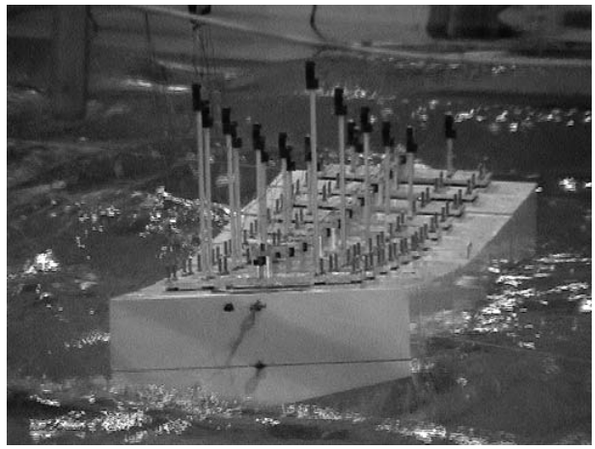

the barge, equipment, measuring procedure and the obtained results is given in [4, 12]. The barge is constructed to be quite flexible in order to expose high level of hydroelastic phenomena. The success of this intention can be seen in Figure 8, where the barge distortion follows more or less the wave surface. The model tests were performed in irregular waves generated by JONSWAP spectra.

Numerical calculation of the barge response to waves is performed for a set of heading angles. For verification of the described methodology and numerical simulation only the transfer functions for $\chi = 60°$ are shown and compared to the measured ones. This particular heading angle was chosen since it includes complete coupling of the rigid and flexible modes of the vertical and horizontal and torsional vibrations, which are highly exited in the case of quartering seas.

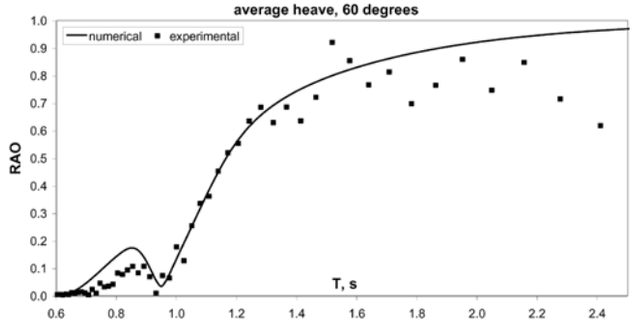

Figure 9 **Average heave transfer function**
Slika 9 **Prosječna prijenosna funkcija poniranja**

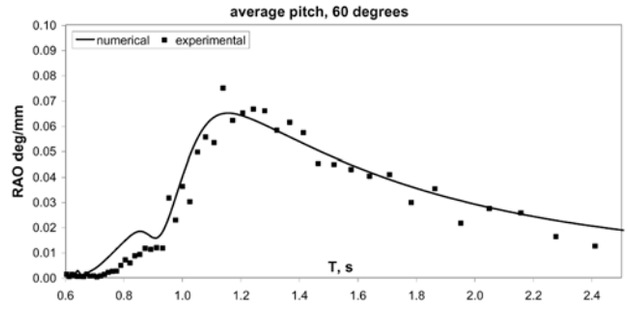

Figure 10 **Average pitch transfer function**
Slika 10 **Prosječna prijenosna funkcija posrtanja**

Figure 11 **Average roll transfer function**
Slika 11 **Prosječna prijenosna funkcija ljuljanja**

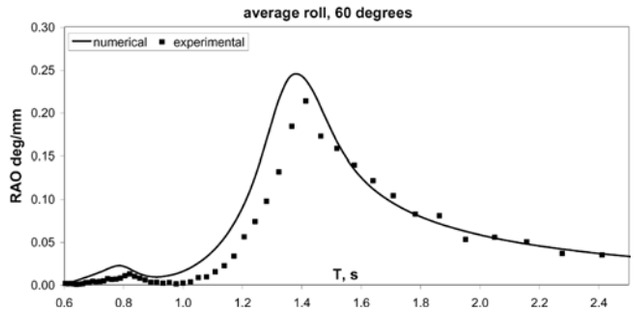

Figures 9, 10 and 11 show RAOs (Response Amplitude Operator-transfer function) in the wave period domain, T, for the average value of heave, pitch and roll respectively, measured at the every second pontoon. In Figures 12, 13 and 14, vertical and horizontal bending and barge torsion are shown. These quantities are defined as difference of the rotation angles at the last and first pontoon.

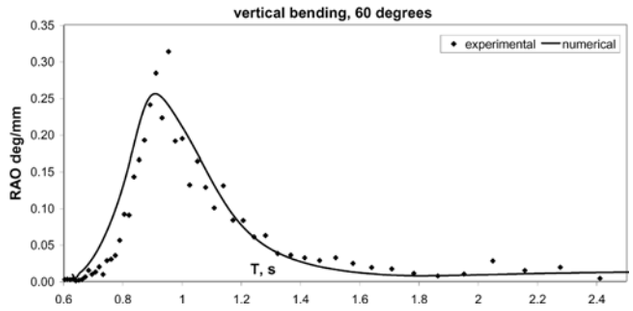

Figure 12 **Vertical bending transfer function**
Slika 12 **Prijenosna funkcija vertikalnog savijanja**

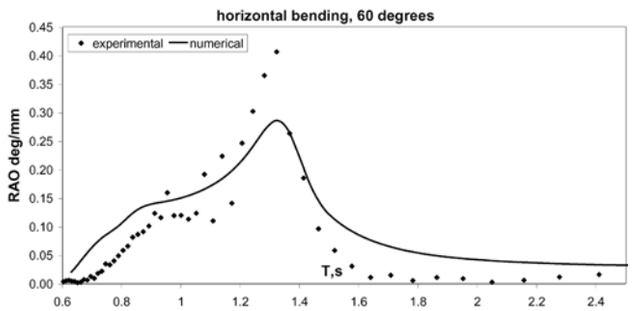

Figure 13 **Horizontal bending transfer function**
Slika 13 **Prijenosna funkcija horizontalnog savijanja**

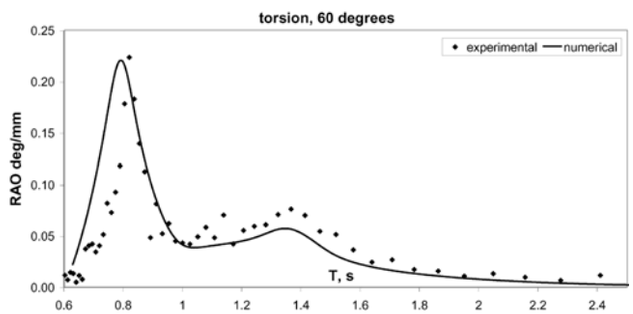

Figure 14 **Torsional transfer function**
Slika 14 **Prijenosna funkcija uvijanja**

RAOs are related to the wave height spectrum. Thus, the heave RAO, as translation motion, converges to unity for higher T values. Contrary, RAOs for all others motions, which are rotational, converge to zero [1].

The relatively large scattering of the measured transfer functions is mostly caused by irregular waves. The obtained numerical results agree quite well with the average of the measured ones. Higher discrepancies between the calculated and measured values occur in area of the response peaks, i.e. at resonances

where damping plays the main role. Figures 9-14 show the final calculation results determined by adjusting damping to achieve minimal discrepancies.

The modal damping is adjusted in such a way that the value of diagonal elements in damping matrix is increased for ca 5%, depending on the type of vibration, i.e. rigid body, vertical vibration and coupled horizontal and torsional vibration. This adaptation can be physically explained. Namely, in the hydroelastic analysis the segmented barge is considered as a monohull. The influence of this assumption on restoring forces and water inertia forces is negligible. However, additional resistance to the pontoon motion is induced between their heads, Figure 15. In the case of an elastic vibration mode the pontoons play as a *shell family on the string with the jet propulsion.* The induced resistance depends on the relative angular velocity of the pontoon adjacent heads.

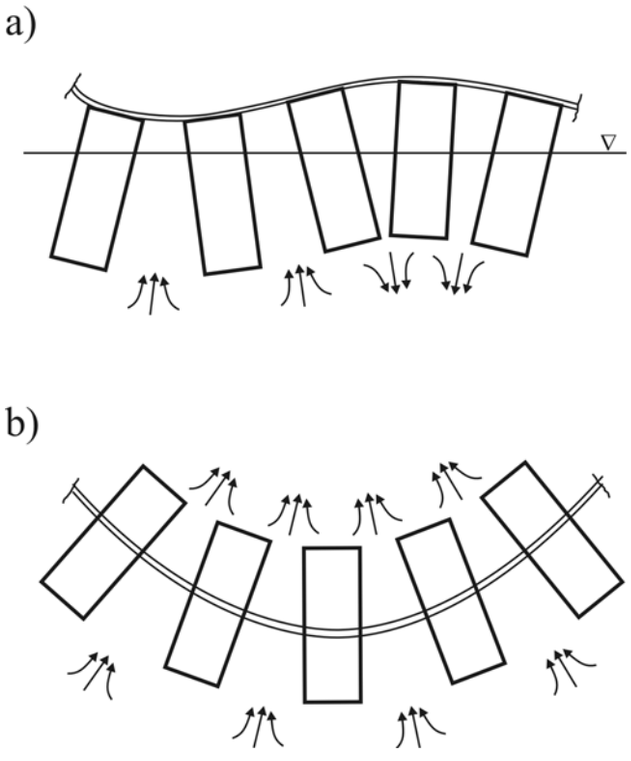

Figure 15 **Pump effect of pontoon oscillations**
a – vertical vibration
b – horizontal vibration
Slika 15 **Pumpni učinak osciliranja pontona**
a – vertikalne vibracije
b – horizontalne vibracije

9 Conclusion

The investigation methodology of hydroelasticity of ship structures is presented. A mathematical model which combines ship geometry, mass distribution, 1D hull model, dry natural vibrations, hydrostatic model and hydrodynamic model is worked out. The numerical procedure and developed computer program are validated for the case of a very flexible barge for which coupling between rigid and elastic modes is highly pronounced as well as coupling between horizontal and torsional vibrations. Quite good agreement between simulated and measured barge response for this very sensitive non-linear experimental model with large amplitudes of rigid and elastic modes of the same order is achieved. Thus, one may conclude that the presented methodology and mathematical model are reliable enough to be applied for hydroelastic analysis of ship structures for which the amplitude ratio of the elastic and rigid modes is somewhat lower.

Application of the developed tool is especially important for hydroelastic analysis of large container ships which are very flexible from torsional point of view, and therefore exposed to the high level of coupling between horizontal and torsional vibrations.

The further development is directed to the investigation of the hydroelastic response to impulsive load, i.e. slamming and whipping, sloshing, underwater explosions etc. in time domain. The final target is to analyse the influence of ship elasticity on wave load in order to check validity and applicability of the present classification rules for large container ships. In the meantime, direct strength calculation as a hydroelastic task should be applied.

References

[1] …:"Principles of Naval Architectures", SNAME, 1988.
[2] HUGHES, O.F.: "Ship Structural Design", SNAME, 1988.
[3] BISHOP, R.E.D., PRICE, W.G.: "Hydroelasticity of Ships", Cambridge University Press, 1979.
[4] REMY, F., MOLIN, B., LEDOUX, A.: "Experimental and numerical study of the wave response of a flexible barge", Hydroelasticity in Marine Technology, Wuxi, China, 2006, p. 255-264.
[5] SALVENSEN, N., TUCK, E.O,. FALTINSEN, O.: "Ship motion and sea loads", Transactions, SNAME, Vol. 70, p. 250-287, 1970.
[6] SENJANOVIĆ, I., GRUBIŠIĆ, R.: "Coupled horizontal and torsional vibration of a ship hull with large hatch openings", Computers & Structures, Vol. 41, No. 2, p. 213-226, 1991.
[7] BATHE, K.J: "Finite Element Procedures", Prentice Hall, 1996.
[8] SENJANOVIĆ, I.: "Finite Element Method in Ship Structures", University of Zagreb, Zagreb, 1998. (in Croatian).
[9] MALENICA, Š., SENJANOVIĆ, I., CHEN, X.B.: "Automatic mesh generation for naval and offshore hydrodynamic simulations", SORTA'04, Plitvice Lakes, Croatia, 2004.
[10] SENJANOVIĆ, I., FAN, Y.: "A finite element formulation of ship cross-sectional stiffness parameters", Brodogradnja 41(1993)1, p. 27-36.
[11] SENJANOVIĆ, I., FAN, Y.: "A higher-order theory of thin-walled girders with application to ship structures", Computers & Structures, 43(1992) 1, p. 31-52.
[12] MALENICA, Š., MOLIN, B., REMY, F., SENJANOVIĆ, I.: "Hydroelastic response of a barge to impulsive and non-impulsive wave load", Hydroelasticity in Marine Technology, Oxford, UK, 2003, p. 107-115.
[13] NAHIN, P.J.: "An Imaginary Tale - The Story of $\sqrt{-1}$ ", Princeton University Press, 1998.
[14] MALENICA, Š.: "Some aspects of hydrostatic calculations in linear seakeeping", The 14th NAV Conference, Palermo, Italy, 2003.
[15] MOLIN, B.: "Hydrostatique d'un corps deformable", Technical note, Ecole Superieure d'Ingenieurs de Marseille, Marseille, France, 2003.

[16] NEWMAN, J.N.: "Wave effects on deformable bodies", Applied Ocean Research 16(1994), p. 47-59.
[17] HUANG, L.L., RIGGS, R.R.: "The hydrostatic stiffness of flexible floating structure for linear hydroelasticity", Marine Structures, 13(2000), p. 91-106.
[18] TOMAŠEVIĆ, S.: "Hydroelastic model of dynamic response of Container ships in waves", Ph. D. Thesis, FSB, Zagreb, 2007. (in Croatian).
[19] SENJANOVIĆ, I., ĆATIPOVIĆ, I., TOMAŠEVIĆ, S.: "Coupled horizontal and torsional vibrations of a flexible barge", Engineering Structures (accepted).
[20] …: "Hydrostar, User's manual", Bureau Veritas, Paris, 2006.
[21] BRONSTEIN, I.N., SEMENDJAJEW, K.A., MUSIOL, G., MÜHLIG, H.: "Mathematical Handbook", Golden marketing - Tehnička knjiga, Zagreb, 2004. (in Croatian).
[22] KREYSZIG, E.: Advanced Engineering Mathematics, John Wiley & Sons, Inc., 1993.
[23] NOVOŽILOV, V.V.: "Thin Shell Theory", P. Noordhoff Ltd., Groningen. The Netherlands, 1964.
[24] SENJANOVIĆ, I.: "Plate and Shell Theory", University of Zagreb, Zagreb, 1998. (in Croatian).

Appendix A

Variation of body surface normal vector

Parametric body surface

A body surface can be represented in the x, y, z - space in implicit, explicit, parametric or vectorial form [21], [22]. In the considered problem the vectorial representation by position vector is preferable (widely used in the shell theory [23], [24])

$$\mathbf{r} = x(u,v)\,\mathbf{i} + y(u,v)\,\mathbf{j} + z(u,v)\,\mathbf{k} \tag{A1}$$

where u and v are parameters that form coordinate mesh on the surface. Therefore, these parameters are called curved or Gauss coordinates.

It is well-known in the differential geometry that the arcs of differential surface are, Figure A1

$$\begin{aligned} \mathrm{d}\,\mathbf{s}_u &= \frac{\partial \mathbf{r}}{\partial u}\mathrm{d}\,u = \left(\frac{\partial x}{\partial u}\mathbf{i} + \frac{\partial y}{\partial u}\mathbf{j} + \frac{\partial z}{\partial u}\mathbf{k}\right)\mathrm{d}\,u \\ \mathrm{d}\,\mathbf{s}_v &= \frac{\partial \mathbf{r}}{\partial v}\mathrm{d}\,v = \left(\frac{\partial x}{\partial v}\mathbf{i} + \frac{\partial y}{\partial v}\mathbf{j} + \frac{\partial z}{\partial v}\mathbf{k}\right)\mathrm{d}\,v \end{aligned} \tag{A2}$$

For differential surface one finds

$$\mathrm{d}\,\mathbf{S} = \mathrm{d}\,\mathbf{s}_u \times \mathrm{d}\,\mathbf{s}_v = \mathbf{N}\,\mathrm{d}\,u\,\mathrm{d}\,v \tag{A3}$$

where components of the normal vector are the following

$$\begin{aligned} N_x &= \frac{\partial y}{\partial u}\frac{\partial z}{\partial v} - \frac{\partial z}{\partial u}\frac{\partial y}{\partial v} \\ N_y &= \frac{\partial z}{\partial u}\frac{\partial x}{\partial v} - \frac{\partial x}{\partial u}\frac{\partial z}{\partial v} \\ N_z &= \frac{\partial x}{\partial u}\frac{\partial y}{\partial v} - \frac{\partial y}{\partial u}\frac{\partial x}{\partial v} \end{aligned} \tag{A4}$$

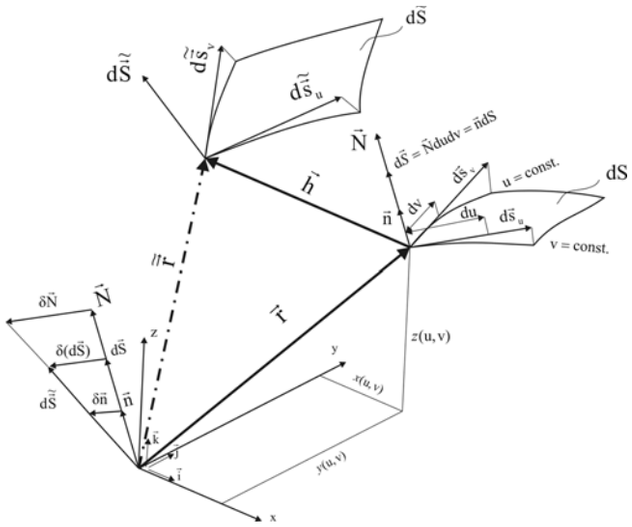

Figure A1 **Definition of normal vector variation δn due to modal deformation h of the parametrically defined body surface**

Slika A1 **Definiranje varijacije normale δn parametarski zadane površine tijela uslijed modalne deformacije h**

If the body surface is deformed by the mode **h**, the deformed surface is represented by the resulting position vector

$$\tilde{\mathbf{r}} = \mathbf{r} + \mathbf{h} \tag{A5}$$

The corresponding arcs read

$$\begin{aligned} \mathrm{d}\,\tilde{\mathbf{s}}_u &= \frac{\partial \tilde{\mathbf{r}}}{\partial u}\mathrm{d}\,u = \left(\frac{\partial \mathbf{r}}{\partial u} + \frac{\partial \mathbf{h}}{\partial u}\right)\mathrm{d}\,u \\ \mathrm{d}\,\tilde{\mathbf{s}}_v &= \frac{\partial \tilde{\mathbf{r}}}{\partial v}\mathrm{d}\,v = \left(\frac{\partial \mathbf{r}}{\partial v} + \frac{\partial \mathbf{h}}{\partial v}\right)\mathrm{d}\,v \end{aligned} \tag{A6}$$

and the deformed differential surface

$$\mathrm{d}\,\tilde{\mathbf{S}} = \mathrm{d}\,\tilde{\mathbf{s}}_u \times \mathrm{d}\,\tilde{\mathbf{s}}_v = \left[\frac{\partial \mathbf{r}}{\partial u}\times\frac{\partial \mathbf{r}}{\partial v} + \frac{\partial \mathbf{h}}{\partial u}\times\frac{\partial \mathbf{r}}{\partial v} + \frac{\partial \mathbf{r}}{\partial u}\times\frac{\partial \mathbf{h}}{\partial v} + \frac{\partial \mathbf{h}}{\partial u}\times\frac{\partial \mathbf{h}}{\partial v}\right]\mathrm{d}\,u\,\mathrm{d}\,v \tag{A7}$$

The first product in (A7) is d**S**, while the last product is a small quantity of higher order and can be therefore neglected. Thus, one finds for variation of differential surface

$$\delta(\mathrm{d}\,\mathbf{S}) = \mathrm{d}\,\tilde{\mathbf{S}} - \mathrm{d}\,\mathbf{S} = \left[\frac{\partial \mathbf{h}}{\partial u}\times\frac{\partial \mathbf{r}}{\partial v} + \frac{\partial \mathbf{r}}{\partial u}\times\frac{\partial \mathbf{h}}{\partial v}\right]\mathrm{d}\,u\,\mathrm{d}\,v = \boldsymbol{\delta}\mathbf{N}\,\mathrm{d}\,u\,\mathrm{d}\,v \tag{A8}$$

The above vector products take form

$$\begin{aligned} \frac{\partial \mathbf{h}}{\partial u}\times\frac{\partial \mathbf{r}}{\partial v} &= \left[\frac{\partial h_y}{\partial u}\frac{\partial z}{\partial v} - \frac{\partial h_z}{\partial u}\frac{\partial y}{\partial v}\right]\mathbf{i} + \left[\frac{\partial h_z}{\partial u}\frac{\partial x}{\partial v} - \frac{\partial h_x}{\partial u}\frac{\partial z}{\partial v}\right]\mathbf{j} + \left[\frac{\partial h_x}{\partial u}\frac{\partial y}{\partial v} - \frac{\partial h_y}{\partial u}\frac{\partial x}{\partial v}\right]\mathbf{k} \\ \frac{\partial \mathbf{r}}{\partial u}\times\frac{\partial \mathbf{h}}{\partial v} &= \left[\frac{\partial h_z}{\partial v}\frac{\partial y}{\partial u} - \frac{\partial h_y}{\partial v}\frac{\partial z}{\partial u}\right]\mathbf{i} + \left[\frac{\partial h_x}{\partial v}\frac{\partial z}{\partial u} - \frac{\partial h_z}{\partial v}\frac{\partial x}{\partial u}\right]\mathbf{j} + \left[\frac{\partial h_y}{\partial v}\frac{\partial x}{\partial u} - \frac{\partial h_x}{\partial v}\frac{\partial y}{\partial u}\right]\mathbf{k} \end{aligned} \tag{A9}$$

Since

$$\mathbf{h} = h_x(x,y,z)\,\mathbf{i} + h_y(x,y,z)\,\mathbf{j} + h_z(x,y,z)\,\mathbf{k} \tag{A10}$$

one can for instance write

$$\frac{\partial h_x}{\partial u}=\frac{\partial h_x}{\partial x}\frac{\partial x}{\partial u}+\frac{\partial h_x}{\partial y}\frac{\partial y}{\partial u}+\frac{\partial h_x}{\partial z}\frac{\partial z}{\partial u} \tag{A11}$$

etc. for the other derivatives of h_x, h_y, h_z per u and v. Furthermore, by substituting those derivatives of type (A11) into (A9) and summing up all terms, one finds according to (A8) variation of the normal vector

$$\begin{aligned}\delta\mathbf{N}=&\left[\left(\frac{\partial h_y}{\partial y}+\frac{\partial h_z}{\partial z}\right)N_x-\frac{\partial h_y}{\partial x}N_y-\frac{\partial h_z}{\partial x}N_x\right]\mathbf{i}+\\&+\left[-\frac{\partial h_x}{\partial y}N_x+\left(\frac{\partial h_x}{\partial x}+\frac{\partial h_z}{\partial z}\right)N_y-\frac{\partial h_z}{\partial y}N_x\right]\mathbf{j}+\\&+\left[-\frac{\partial h_x}{\partial z}N_x-\frac{\partial h_y}{\partial z}N_y+\left(\frac{\partial h_x}{\partial x}+\frac{\partial h_y}{\partial y}\right)N_x\right]\mathbf{k}\end{aligned} \tag{A12}$$

as it is elaborated in [14]. Since

$$\delta\mathbf{N}\,\mathrm{d}u\,\mathrm{d}v=\delta\mathbf{n}\,\mathrm{d}S \tag{A13}$$

the same form of expression (A12) is also valid for the variation of the unit vector, δn, with components n_x, n_y and n_z.

Explicit body surface

Body surface can also be represented in one of the following vectorial forms

$$\begin{aligned}\mathbf{r}&=X(y,z)\mathbf{i}+y\,\mathbf{j}+z\,\mathbf{k}\\\mathbf{r}&=x\,\mathbf{i}+Y(x,z)\,\mathbf{j}+z\,\mathbf{k}\\\mathbf{r}&=x\,\mathbf{i}+y\,\mathbf{j}+Z(x,y)\,\mathbf{k}\end{aligned} \tag{A14}$$

where the second form is conventional in naval architecture, Section 3.1. Arcs of differential surface in the first case yield

$$\begin{aligned}\mathrm{d}\mathbf{s}_1&=\frac{\partial\mathbf{r}}{\partial y}\mathrm{d}y=\left(\frac{\partial X}{\partial y}\mathbf{i}+\mathbf{j}\right)\mathrm{d}y\\\mathrm{d}\mathbf{s}_2&=\frac{\partial\mathbf{r}}{\partial z}\mathrm{d}z=\left(\frac{\partial X}{\partial z}\mathbf{i}+\mathbf{k}\right)\mathrm{d}z\end{aligned} \tag{A15}$$

Differential surface reads

$$\mathrm{d}\mathbf{S}=\mathrm{d}\mathbf{s}_1\times\mathrm{d}\mathbf{s}_2=\left(\mathbf{i}-\frac{\partial X}{\partial y}\mathbf{j}-\frac{\partial X}{\partial z}\mathbf{k}\right)\mathrm{d}y\,\mathrm{d}z=\mathbf{N}^x\mathrm{d}S_x=\mathbf{n}\,\mathrm{d}S \tag{A16}$$

where $\mathrm{d}S_x=\mathrm{d}y\,\mathrm{d}z$, i.e. orthogonal projection of $\mathrm{d}S$ onto y, z plane, $\mathbf{N}^x$ is the corresponding normal vector while $\mathbf{n}$ is the unit normal vector.

In the second and third surface representation (A14) in a similar way one finds

$$\mathrm{d}\mathbf{S}=\left(\frac{\partial Y}{\partial x}\mathbf{i}-\mathbf{j}+\frac{\partial Y}{\partial z}\mathbf{k}\right)\mathrm{d}x\,\mathrm{d}z=\mathbf{N}^y\mathrm{d}S_y=\mathbf{n}\,\mathrm{d}S \tag{A17}$$

$$\mathrm{d}\mathbf{S}=\left(-\frac{\partial Z}{\partial x}\mathbf{i}-\frac{\partial Z}{\partial y}\mathbf{j}+\mathbf{k}\right)\mathrm{d}x\,\mathrm{d}y=\mathbf{N}^z\mathrm{d}S_z=\mathbf{n}\,\mathrm{d}S \tag{A18}$$

The corresponding quantities for the third case of body surface definition are shown in Figure A2.

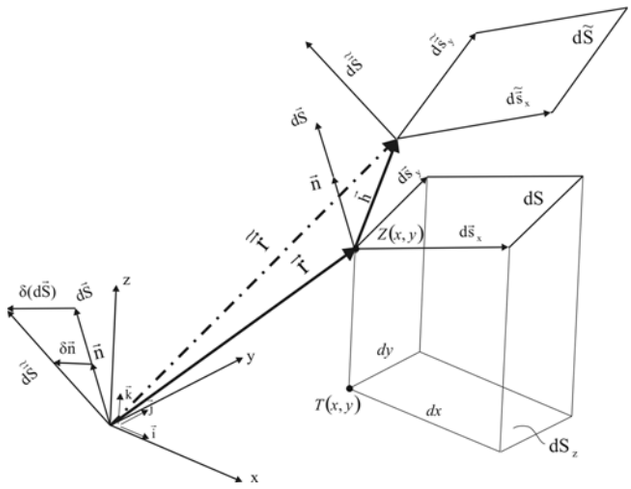

Figure A2 **Definition of normal vector variation $(\delta\mathbf{n})^z$ due to modal deformation h for the explicitly defined body surface $Z = Z(x, y)$**

Slika A2 **Definiranje varijacije normale $(\delta\mathbf{n})^z$ eksplicitno zadane površine tijela $Z = Z(x, y)$ uslijed modalne deformacije h**

The deformed body surface by mode $\mathbf{h}$ is represented by vector

$$\tilde{\mathbf{r}}=\mathbf{r}+\mathbf{h} \tag{A19}$$

In the first surface definition (A14) one can write for arcs of differential element of deformed surface

$$\begin{aligned}\mathrm{d}\tilde{\mathbf{s}}_y&=\frac{\partial\tilde{\mathbf{r}}}{\partial y}\mathrm{d}y=\left(\frac{\partial\mathbf{r}}{\partial y}+\frac{\partial\mathbf{h}}{\partial y}\right)\mathrm{d}y\\\mathrm{d}\tilde{\mathbf{s}}_z&=\frac{\partial\tilde{\mathbf{r}}}{\partial z}\mathrm{d}z=\left(\frac{\partial\mathbf{r}}{\partial z}+\frac{\partial\mathbf{h}}{\partial z}\right)\mathrm{d}z\end{aligned} \tag{A20}$$

Differential element is defined as follows

$$\mathrm{d}\tilde{\mathbf{S}}=\mathrm{d}\tilde{\mathbf{s}}_y\times\mathrm{d}\tilde{\mathbf{s}}_z=\left[\left(\frac{\partial\mathbf{r}}{\partial y}\times\frac{\partial\mathbf{r}}{\partial z}\right)+\left(\frac{\partial\mathbf{h}}{\partial y}\times\frac{\partial\mathbf{r}}{\partial z}\right)+\left(\frac{\partial\mathbf{r}}{\partial y}\times\frac{\partial\mathbf{h}}{\partial z}\right)+\left(\frac{\partial\mathbf{h}}{\partial y}\times\frac{\partial\mathbf{h}}{\partial z}\right)\right]\mathrm{d}y\,\mathrm{d}z \tag{A21}$$

Similarly to the parametric representation of body surface, the first product in (A21) represents differential element of the undeformed surface (A16), the last product is a small negligible quantity of higher order, while the second and third products are related to the variation of differential element due to modal deformation. Thus,

$$\delta(\mathrm{d}\mathbf{S})=\mathrm{d}\tilde{\mathbf{S}}-\mathrm{d}\mathbf{S}=\left(\frac{\partial\mathbf{h}}{\partial y}\times\frac{\partial\mathbf{r}}{\partial z}+\frac{\partial\mathbf{r}}{\partial y}\times\frac{\partial\mathbf{h}}{\partial z}\right)\mathrm{d}S_x \tag{A22}$$

Similar expressions can be derived for the other two definitions of body surface (A14)

$$\delta(\mathrm{d}\mathbf{S}) = \left(\frac{\partial \mathbf{h}}{\partial x}\times\frac{\partial \mathbf{r}}{\partial z} + \frac{\partial \mathbf{r}}{\partial x}\times\frac{\partial \mathbf{h}}{\partial z}\right)\mathrm{d}S_y \tag{A23}$$

$$\delta(\mathrm{d}\mathbf{S}) = \left(\frac{\partial \mathbf{h}}{\partial x}\times\frac{\partial \mathbf{r}}{\partial y} + \frac{\partial \mathbf{r}}{\partial x}\times\frac{\partial \mathbf{h}}{\partial y}\right)\mathrm{d}S_z \tag{A24}$$

By substituting (A14) into (A22), (A23) and (A24) respectively and taking into account relation

$$\delta(\mathrm{d}\mathbf{S}) = \delta\mathbf{n}\,\mathrm{d}S \tag{A25}$$

and (A10), one finds the following three expressions for the normal vector variation depending on the body surface definition (A14)

$$(\delta\mathbf{n})^x = \left(\frac{\partial h_y}{\partial y}+\frac{\partial h_z}{\partial z}\right)n_x\mathbf{i} + \left(-\frac{\partial h_x}{\partial y}n_x + \frac{\partial h_z}{\partial z}n_y - \frac{\partial h_z}{\partial y}n_z\right)\mathbf{j} + \left(-\frac{\partial h_x}{\partial z}n_x - \frac{\partial h_y}{\partial z}n_y + \frac{\partial h_y}{\partial y}n_z\right)\mathbf{k} \tag{A26}$$

$$(\delta\mathbf{n})^y = \left(\frac{\partial h_z}{\partial z}n_x - \frac{\partial h_y}{\partial x}n_y - \frac{\partial h_z}{\partial x}n_z\right)\mathbf{i} + \left(\frac{\partial h_x}{\partial x}+\frac{\partial h_z}{\partial z}\right)n_y\mathbf{j} + \left(-\frac{\partial h_x}{\partial z}n_x - \frac{\partial h_y}{\partial z}n_y + \frac{\partial h_x}{\partial x}n_z\right)\mathbf{k} \tag{A27}$$

$$(\delta\mathbf{n})^z = \left(\frac{\partial h_y}{\partial y}n_x - \frac{\partial h_y}{\partial x}n_y - \frac{\partial h_z}{\partial x}n_z\right)\mathbf{i} + \left(-\frac{\partial h_x}{\partial y}n_x + \frac{\partial h_x}{\partial x}n_y - \frac{\partial h_z}{\partial y}n_z\right)\mathbf{j} + \left(\frac{\partial h_x}{\partial x}+\frac{\partial h_y}{\partial y}\right)n_z\mathbf{k} \tag{A28}$$

Figure A3 **A Venn diagram for variation of unit normal vector in explicitly represented body surface**
Slika A3 **Vennov dijagram varijacije jedinične normale eksplicitno zadane površine tijela**

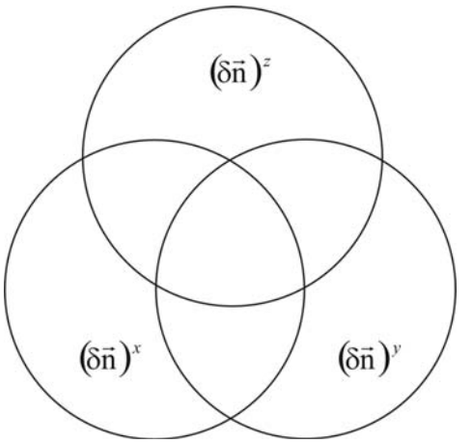

The derived expressions are different in spite of the fact that they should represent the same quantity. Almost a half of their terms are common. Due to practical reason, a unified expression should be formulated. If we want to keep all essential terms of formulae (A26), (A27) and (A28) in such a formulation without their repeating, then let us refer to the mathematical logic and apply the set theory [21], [22]. In that case the unified expression for variation of normal vector is represented with the union of sets (A26), (A27) and (A28)

$$\delta\mathbf{n} = (\delta\mathbf{n})^x \cup (\delta\mathbf{n})^y \cup (\delta\mathbf{n})^z \tag{A29}$$

which is illustrated by Venn diagram in Figure A3. It is interesting to point out that the following relation also exists in the considered case

$$\delta\mathbf{n} = \frac{1}{2}\left[(\delta\mathbf{n})^x + (\delta\mathbf{n})^y + (\delta\mathbf{n})^z\right] \tag{A30}$$

Appendix B

Barge restoring stiffness for vertical vibration

As specified in Section 8.3, the barge hydroelastic analysis is performed by taking into account 6 rigid body modes, 5 dry vertical modes, and 5 dry coupled horizontal and torsional modes. These modes in three sets are denoted with index i = 1, 2...6; 7, 8...11; 12, 13...16.

Only static pressure acting on the barge bottom and the barge front and aft heads is relevant for the barge hydrostatic stiffness in the case of vertical vibration. The pressure forces on the barge sides and the adjacent pontoon heads are in equilibrium and therefore cancelled. For the bottom panels the normal vector is $\mathbf{n} = \mathbf{k}$, while for the aft and fore head panels $\mathbf{n} = \pm\,\mathbf{i}$ respectively. The origin of the coordinate system is located at the waterplane below the centre of gravity, Figure B1.

According to (11) the bottom elastic mode yields

$$\mathbf{h}_{iK} = \varphi_i(z_N + T)\mathbf{i} + w_i\mathbf{k}\ ,\ i = 7,\ 8... \tag{B1}$$

Figure B1 **Coordinates of actual points for restoring stiffness determination**
Slika B1 **Koordinate bitnih točaka za određivanje povratne krutosti**

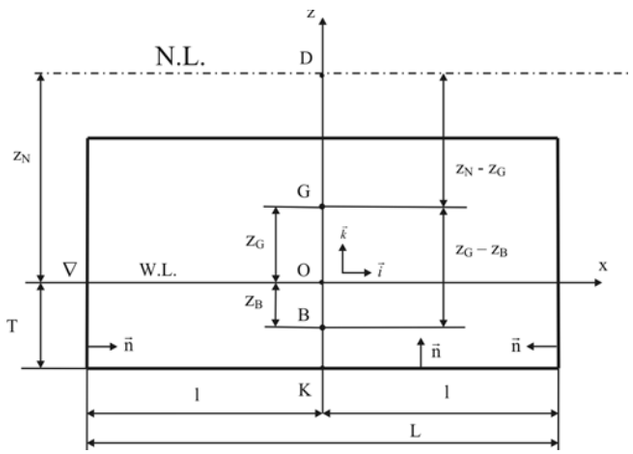

while at the level of the centre of gravity one finds

$$\mathbf{h}_{iG} = \varphi_i(z_N - z_G)\mathbf{i} + w_i\mathbf{k}\ ,\ i = 7, 8... \tag{B2}$$

where w_i is the barge deflection and φ_i rotation of cross-section.

By employing expressions (32), (33) and (34) for hydrostatic stiffness, and (38) for gravity contribution, the following formulae for the elements of the restoring matrix are derived, where $i, j = 7, 8...$

Pressure:

$$C_{ij}^{Hp} = \rho g B \int_{-l}^{l} w_j w_i \,\mathrm{d}x \tag{B3}$$

Modes and normal vector:

$$C_{ij}^{Hhn} = -\rho g BT(z_N + T)\int_{-l}^{l} \frac{\partial \varphi_j}{\partial x} w_i \,\mathrm{d}x \tag{B4}$$

Gravity, $m = \rho BT$:

$$C_{ij}^{m} = \rho g BT(z_N - z_G)\int_{-l}^{l} \varphi_j \varphi_i \,\mathrm{d}x \tag{B5}$$

where $l = L/2$, and L, B, T are the barge length, breadth and draught, respectively.

For the barge heads one finds according to (11), (32), (33) and (34)

$$C_{ij}^{Hp} = r_p\left[w_j(l)\varphi_i(l) - w_j(-l)\varphi_i(-l)\right] \tag{B6}$$

$$C_{ij}^{Hh} = r_{h_1}\left\{r_{h_2}\left[\varphi_j(l)\frac{\partial\varphi_i(l)}{\partial x} - \varphi_j(-l)\frac{\partial\varphi_i(-l)}{\partial x}\right] - \left[w_j(l)\varphi_i(l) - w_j(-l)\varphi_i(-l)\right]\right\} \tag{B7}$$

$$C_{ij}^{Hn} = r_n\left[\varphi_j(l)w_i(l) - \varphi_j(-l)w_i(-l)\right] \tag{B8}$$

where

$$\begin{aligned} r_p &= -\rho g BT\left(z_N + \frac{T}{2}\right) \\ r_{h_1} &= \rho g \frac{BT^2}{2}, \quad r_{h_2} = \frac{T^2}{2} + \frac{4}{3}z_N T + z_N^2 \\ r_n &= \rho g \frac{BT^2}{2} \end{aligned} \tag{B9}$$

The constitution of the hydrostatic and gravity coefficients indicates that the restoring force depends not only on the barge deflection w and cross-section rotation $\varphi = \mathrm{d}w/\mathrm{d}x$, but also on the curvature $\kappa = \mathrm{d}^2w/\mathrm{d}x^2$ that is of low effect.

The above formulae, derived for elastic modes, are general and therefore applicable for rigid body modes, as well as for their coupling with elastic modes. The corresponding indexes for rigid body modes are $i, j = 3, 5$, while for the coupling modes $i = 3, 5$ and $j = 7, 8...$, and vice versa i.e. $i = 7, 8...$ and $j = 3, 5$.

In addition, it is interesting to determine the restoring coefficients for rigid body modes. Thus, one finds for heave, where $w_3 = 1$, $\varphi_3 = 0$:

Bottom:

$$C_{33}^{Hp} = \rho g LB, \quad C_{33}^{Hhn} = C_{33}^{m} = 0 \tag{B10}$$

Heads:

$$C_{33}^{Hp} = C_{33}^{Hhn} = 0 \tag{B11}$$

It is obvious that the total restoring coefficient $C_{33} = \rho g LB$ is equal to that determined by the ship hydrostatics, Eq. (40), since LB is waterplane area, A_{WL}.

The pitch mode yields: $w_5 = x$, $\varphi_5 = 1$, where $-l \le x \le l$. The corresponding coefficients are the following:

Bottom:

$$\begin{aligned} C_{55}^{Hp} &= \rho g \frac{BL^3}{12} \\ C_{55}^{Hhn} &= 0 \\ C_{55}^{m} &= \rho g LBT(z_N - z_G) \end{aligned} \tag{B12}$$

Heads:

$$\begin{aligned} C_{55}^{Hp} &= -\rho g LBT\left(z_N + \frac{T}{2}\right) \\ C_{55}^{Hh} &= -\rho g \frac{LBT^2}{2} \\ C_{55}^{Hn} &= \rho g \frac{LBT^2}{2} \end{aligned} \tag{B13}$$

Since $BL^3/12 = I_{WLY}$ is longitudinal moment of inertia of waterplane area and $LBT = V$ is volume of displacement, the restoring coefficient yields

$$C_{55} = \rho g\left[I_{WLY} - V\left(\frac{T}{2} + z_G\right)\right] \tag{B14}$$

It is identical to the hydrostatic expression (42), since the coordinate of the centre of buoyancy reads $z_B = -T/2$. The coordinate of neutral line, z_N, is cancelled in C_{55} and that is physically correct for rigid body modes.

Concerning coefficients of mixed modes, w_3 and w_5, their values are zero since the modes are orthogonal. As a result, the restoring coefficients yield $C_{35} = C_{53} = 0$.